World Academy of Science, Engineering and Technology
International Journal of Aerospace and Mechanical Engineering
Vol:17, No:10, 2023

Magnetoplasmadynamic Thruster Design and Characteristics

A. Almuwallad

***Abstract*—**The magnetoplasmadynamic (MPD) thruster is classified as an electric propulsion system and consists of two metal electrodes separated by an insulator. A high-current electric arc is driven between electrodes to ionize the injected propellant between electrodes for plasma creation. At the same time, a magnetic field is generated by the electric current returning to the power supply. This magnetic field interacts with the electric current flowing through the plasma to produce thrust. This paper compares the performance of MPD thrusters when using three different propellants (methane, nitrogen, and propane) at varying input mass flow rates. Methane provided the best performance, and nitrogen performed better than propane. In addition, when using the same parameters, the thruster with a divergent nozzle performed better than the thruster with a constant nozzle.

***Keywords*—**Magnetoplasmadynamic thruster, electric propulsion, propellant, plasma.

I. Introduction

GIVEN the technological development in the space field, using highly efficient advanced propulsion systems has become necessary. Therefore, electric propulsion (EP) has become one of the most basic options for space propulsion because it has overcome chemical propulsion in missions concerning space applications, especially deep-space exploration. In general, the term EP refers to propulsion systems that use electricity to generate significant exhaust velocity, which reduces the propellant required for a space mission compared to other conventional propulsion methods, as shown in Fig. 1.

The science and technology of EP include a wide variety of strategies that have been subdivided into the following three types based on the acceleration mechanism [1], [2]:

- electrothermal propulsion system;
- electrostatic propulsion system; and
- electromagnetic propulsion system.

This paper focuses on the MPD thruster, which is currently the most potent form of EP (see Table I) and is classified as an electromagnetic propulsion system [2]-[4]. It consists of two metal electrodes: a central cathode surrounded by an anode shell and a propellant injected between them.

The MPD thruster is operated by applying the electric and magnetic fields perpendicularly to each other across plasma, as shown in Fig. 2. The resulting current density ($\vec{J}$) flowing in the direction of the laid electric field ($\vec{E}$) gives rise to Lorentz force ($\vec{J} \times \vec{B}$), which accelerates the plasma out of the thruster channel. Due to the conservation of momentum, the associated reaction force accelerates the rocket in the direction opposite the plasma flow [1], [5], [6].

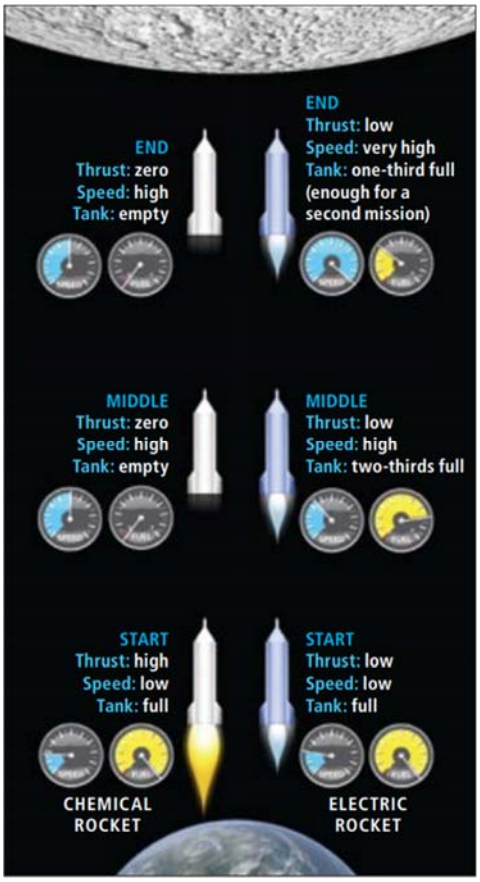

Fig. 1 Chemical rocket vs. electric rocket [6]

TABLE I
Specific Impulse of Different Propulsion Technologies

Technology	I_{sp} (s)	η_t (%)	Input Power (kw)
Cold gas	50 - 75	---	---
Chemical (monopropellant)	150 - 225	---	---
Chemical (bipropellant)	300 - 450	---	---
Resistojets	250 - 400	65 - 90	0.5 - 5
Arcjets	400 - 1800	30 - 50	0.7 - 100
Ion thrusters	2500 - 5000	40 - 80	0.8 - 8
Hall thrusters	1200 - 4000	35 - 60	0.7 - 10
Pulsed Plasma thrusters	700 - 1800	7 - 13	0.1 - 0.7
Helicon Thrusters	500 - 2000	10 - 40	0.05 - 50
MPD Thrusters	1000 - 7000	≤ 40	1 - 1000

A. Almuwallad is with King Abdulaziz University, Jeddah, Saudi Arabia (e-mail: a.almuwallad16@gmail.com).

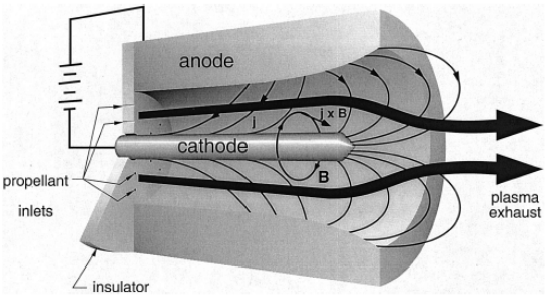

Fig. 2 Schematic of MPD thruster

II. Materials and Methods

The present study was divided into two parts: theoretical and experimental. In the beginning, theoretical calculations were employed to examine the performance of the MPD thruster; then, measurements were made to examine the thruster's performance experimentally. The pre-experiment steps and experiment setup are presented herein, with details about the test equipment used.

The main variables adopted in the present study are shown in Table II.

TABLE II
Main Variables

Variable	Value
Thruster Efficiency	0.1
Current (A)	5000
Mass Flow Rate (kg/s)	0.006
Electron Temperature (eV)	5
M_{atomp} of Methan (Amu)	16.043

A. Theoretical Part

As shown in Table III, the MPD thruster was modeled with different exhaust geometries to study the changes inside the thruster channel and to understand the basic parameters of the plasma acceleration process.

TABLE III
Dimensions of Exhaust Geometries

Variable	Constant Nozzle	Divergent Nozzle
Inlet Anode Radius	1.25 cm	1.25 cm
Outlet Anode Radius	1.25 cm	1.5 cm
Cathode Radius	0.4 cm	0.4 cm
Length	Length depends on variables	

It is crucial to identify the following input variables before listing the mathematical equations:

- cathode radius (r_c);
- anode radius (r_a);
- current (i);
- mass flow rate ($\dot{m}$); and
- thruster length (L_Z).

The magnetic field at the entry of the thruster channel (B_0) can be calculated by integrating Ampere's law.

$$\frac{dB}{dZ} = -\mu_0\, j, \tag{1}$$

where B_0 at $Z = 0$, and integrating between $Z = 0$ and $Z = L_Z$.

$$\int_0^{L_Z} j\, d_Z = \frac{B_0\, L_y}{\mu_0} = i \tag{2}$$

This leads to:

$$B_0 = \frac{\mu_0\, i}{L_y}, \tag{3}$$

where μ_0 is the magnetic permeability of vacuum ($\mu_0 = 4\,\pi\, 10^{-7}$) and $L_y = \pi\,(r_a + r_c)$.

The momentum conservation equation integrated and used (1) to determine the velocity value along the thruster channel.

$$\frac{\dot{m}}{A}\,\frac{du}{dZ} = j\, B, \text{ and} \tag{4}$$

$$u = \frac{A}{2\,\mu_0\,\dot{m}}\,(B_0^2 - B^2), \tag{5}$$

where A is the thruster channel area.

The exhaust velocity value can be found using (5) when imposing that the value of $B = 0$ at $Z = L_Z$.

$$u_e = \frac{A}{2\,\mu_0\,\dot{m}}\,(B_0^2) = \frac{T}{\dot{m}}, \tag{6}$$

where T in (6) represents the thrust and can be calculated as:

$$T = \frac{B_0^2\, A}{2\,\mu_0}. \tag{7}$$

The thrust result can be compared to Maecker's law.

$$T_{Maecker} \approx T$$
$$T_{Maecker} = \frac{\mu_0\, i^2}{4\,\pi}\left(\ln\left(\frac{r_a}{r_c}\right) + \frac{3}{4}\right) \tag{8}$$

E_y represents the electric field in (9):

$$E_y = \frac{V}{L_x}, \tag{9}$$

where V is the voltage and $L_x = r_a - r_c$.

The current density (j) can be calculated based on Ohm's law:

$$j = \sigma\,(E_y - \acute{E}), \tag{10}$$

where σ is the scalar conductivity for plasma and $\acute{E}$ is the induced electric field ($\acute{E} = u\, B$).

Concluding with the equations defining the model, (10) and (1) must be used as (11) to find the thruster channel length (L_Z) when imposing the value of $B = 0$. In addition, (11) can be used to study the u, B, and j values along the thruster channel, as shown in Figs. 3 and 4 [7].

$$\frac{dB}{dZ} = -\mu_0\, j = -\mu_0\,\sigma\left[E_y - \left(\frac{A\,B}{2\,\mu_0\,\dot{m}}\right)(B_0^2 - B^2)\right] \tag{11}$$

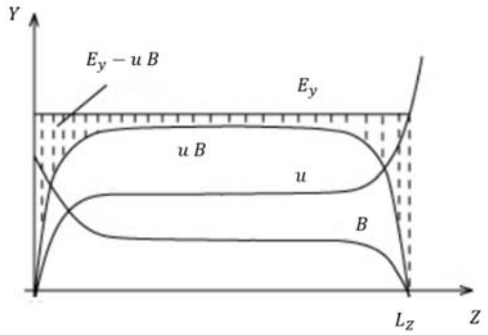

Fig. 3 Velocity, magnetic field, electric field, and induced electric field along the thruster channel

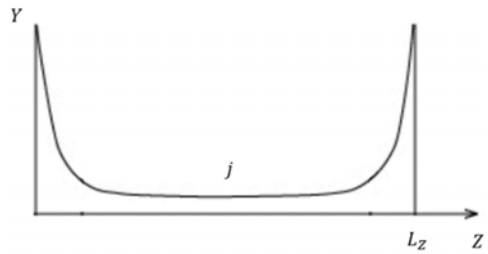

Fig. 4 Current density along the thruster channel

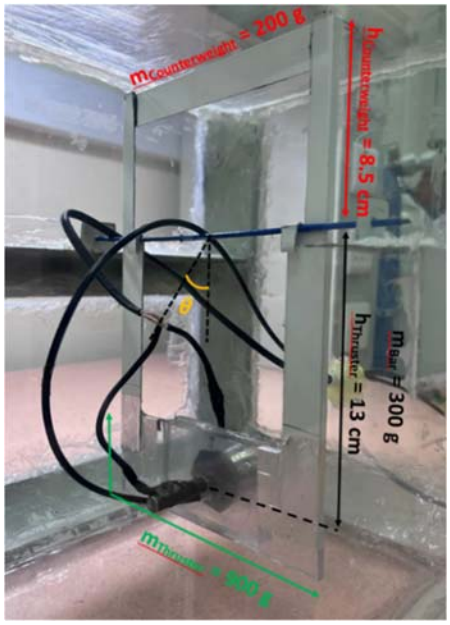

Fig. 5 Suspended pendulum

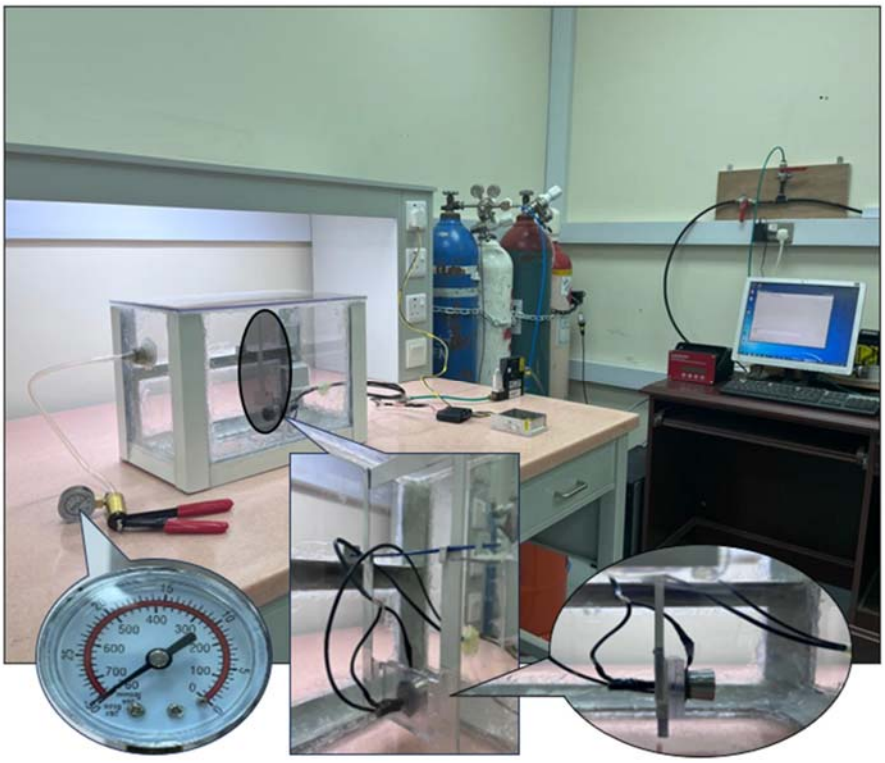

Fig. 6 Experiment setup

B. Experimental Part

The experiment was performed in two phases. Each phase represented a different exhaust geometry. The MPD thruster with a constant nozzle was used in the first phase, while the MPD thruster with a divergent nozzle was used in the second phase. Tables II and III show the dimensions of the built thrusters. They were mounted on a suspended pendulum, as shown in Fig. 5. The pendulum interacted with the thrust force generated by the thrusters, causing it to move at an angle. The angular position was measured and then used in (12) to calculate T [8], [9]:

$$F_{Thrust} = \left(W_{Thruster} + W_{Bar} - W_{Counterweight}\frac{h_{Counterweight}}{h_{Thruster}}\right)\sin\theta \quad (12)$$

Then, plasma was generated using a 5 V power supply and transformers to provide the required i. Finally, the thruster mounted on the suspended pendulum was placed inside a vacuum chamber to simulate the space properties. Correct results were provided as shown in the experiment setup in Fig. 6.

The propellant cylinders were connected to the mass flow rate controller (MFC) to control $\dot{m}$. They were then connected to the control module linked to a computer program. The MFC was managed by a dedicated computer, allowing for control of propellant $\dot{m}$. The output of the MFC was connected to the channel inlet.

III. Results and Discussion

Mission planners and propulsion system designers focus on T, I_{sp}, and u_e. These critical parameters reflect the MPD thruster's performance. Thus, the performance of MPD thrusters using different $\dot{m}$ values and propellants (propane, nitrogen, and methane) was compared in the present study.

A. Theoretical Results

Based on the equations in Section II, MATLAB was utilized to calculate T, I_{sp}, and u_e for MPD thrusters with different exhaust geometries. Table IV and Fig. 7 show the results for the MPD thruster with a constant nozzle, while Table V and Fig. 8 show the results for the MPD thruster with a divergent nozzle.

TABLE IV
Theoretical Results for the MPD Thruster with a Constant Nozzle (L_Z = 3.02)

P	$\dot{m}$ (kg/s)	T (N)	u_e (m/s)	I_{sp} (s)
Propane (C_3H_8)	0.002	2.5758	1287.9	131.2844037
	0.004	2.5758	643.95	65.64220183
	0.006	2.5554	425.9	43.41488277
	0.008	2.3608	295.1	30.08154944
	0.01	2.1636	216.36	22.05504587
	0.015	1.7808	118.72	12.1019368
	0.02	1.506	75.3	7.675840979
	0.025	1.3534	54.136	5.518450561
Nitrogen (N_2)	0.002	2.5758	1287.9	131.2844037
	0.004	2.5758	643.95	65.64220183
	0.006	2.5707	428.45	43.67482161
	0.008	2.4218	302.725	30.85881753
	0.01	2.2388	223.88	22.8216106
	0.015	1.847	123.1333333	12.55181787
	0.02	1.5951	79.755	8.129969419
	0.025	1.4075	56.3	5.739041794
Methane (CH_4)	0.002	2.5758	1287.9	131.2844037
	0.004	2.5758	643.95	65.64220183
	0.006	2.5758	429.3	43.76146789
	0.008	2.4727	309.0875	31.50739042
	0.01	2.312	231.2	23.56778797
	0.015	1.9318	128.7866667	13.12810058
	0.02	1.6954	84.77	8.641182467
	0.025	1.5003	60.012	6.117431193

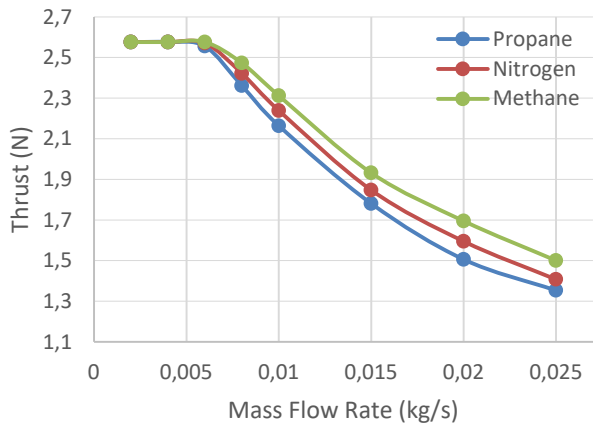

Fig. 7 Thrust vs. mass flow rate for the MPD thruster with a constant nozzle (L_Z = 3.02)

TABLE V
Theoretical Results for the MPD Thruster with a Divergent Nozzle (L_Z = 1.42)

P	$\dot{m}$ (kg/s)	T (N)	u_e (m/s)	I_{sp} (s)
Propane (C_3H_8)	0.002	3.8384	1919.2	195.637105
	0.004	3.8384	959.6	97.8185525
	0.006	3.8157	635.95	64.82670744
	0.008	3.634	454.25	46.30479103
	0.01	3.4377	343.77	35.04281346
	0.015	2.9653	197.6866667	20.15154604
	0.02	2.6469	132.345	13.49082569
	0.025	2.39	95.6	9.745158002
Nitrogen (N_2)	0.002	3.8384	1919.2	195.637105
	0.004	3.8384	959.6	97.8185525
	0.006	3.8302	638.3666667	65.07305471
	0.008	3.6848	460.6	46.9520897
	0.01	3.5104	351.04	35.78389399
	0.015	3.0743	204.9533333	20.89228678
	0.02	2.7255	136.275	13.89143731
	0.025	2.4566	98.264	10.01671764
Methane (CH_4)	0.002	3.8384	1919.2	195.637105
	0.004	3.8384	959.6	97.8185525
	0.006	3.8384	639.7333333	65.21236833
	0.008	3.7475	468.4375	47.75101937
	0.01	3.5758	357.58	36.45056065
	0.015	3.1761	211.74	21.58409786
	0.02	2.849	142.45	14.52089704
	0.025	2.5947	103.788	10.57981651

B. Experiment Results

Table VI and Fig. 9 show the results for the MPD thruster with a constant nozzle, while Table VII and Fig. 10 show the results for the MPD thruster with a divergent nozzle.

C. Discussion

The study results show that the propellant with a lower molecular weight performs better. Methane performed better than the other propellants, and nitrogen performed better than propane. As the acceleration of the propellant in this type of propulsion occurs due to ionization, it is necessary to calculate the thruster's L_Z accurately. As $\dot{m}$ increases, it needs a greater L_Z to fully ionize the propellant, leading to the greatest thrust.

Alternatively, a higher i value can compensate for the difference in L_Z.

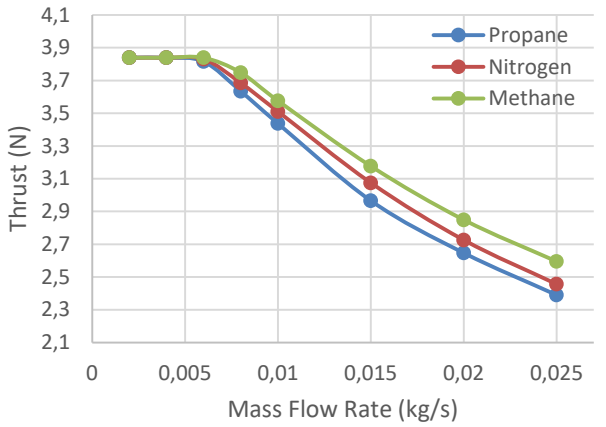

Fig. 8 Thrust vs. mass flow rate for the MPD thruster with a divergent nozzle (L_Z = 1.42)

TABLE VI
EXPERIMENT RESULTS FOR THE MPD THRUSTER WITH A CONSTANT NOZZLE (L_Z = 3.02)

P	$\dot{m}$ (kg/s)	θ	T (N)	u_e (m/s)	I_{sp} (s)
Propane (C_3H_8)	0.002	11.2	2.6089856	1304.4928	132.97582
	0.004	11	2.5629757	640.74394	65.315386
	0.006	10.8	2.5169346	419.48910	42.761376
	0.008	9.8	2.2862801	285.78502	29.132010
	0.01	9	2.1012518	210.12518	21.419488
	0.015	7.2	1.6834952	112.23301	11.440674
	0.02	6.2	1.4506639	72.533198	7.3938020
	0.025	5.5	1.2874148	51.496595	5.2493981
Nitrogen (N_2)	0.002	10.9	2.5399590	1269.9795	129.45764
	0.004	11	2.5629757	640.74394	65.315386
	0.006	10.8	2.5169346	419.48910	42.761376
	0.008	10.3	2.4016988	300.21235	30.602686
	0.01	9.4	2.1938194	219.38194	22.363093
	0.015	7.7	1.7997230	119.98153	12.230533
	0.02	6.5	1.5205629	76.028149	7.7500661
	0.025	5.8	1.3574037	54.296149	5.5347756
Methane (CH_4)	0.002	11	2.5629757	1281.4878	130.63077
	0.004	11	2.5629757	640.74394	65.315386
	0.006	10.8	2.5169346	419.48910	42.761376
	0.008	10.6	2.4708628	308.85785	31.483981
	0.01	9.8	2.2862801	228.62801	23.305608
	0.015	8	1.8693945	124.62630	12.704006
	0.02	7	1.636967	81.848388	8.3433627
	0.025	6.3	1.4739681	58.958725	6.0100638

When the results of the two phases were compared, it was observed that the second phase outperformed the first. In addition, it was observed during the experiments that j in the second phase was greater than that in the first phase, which was predicted in the theoretical results.

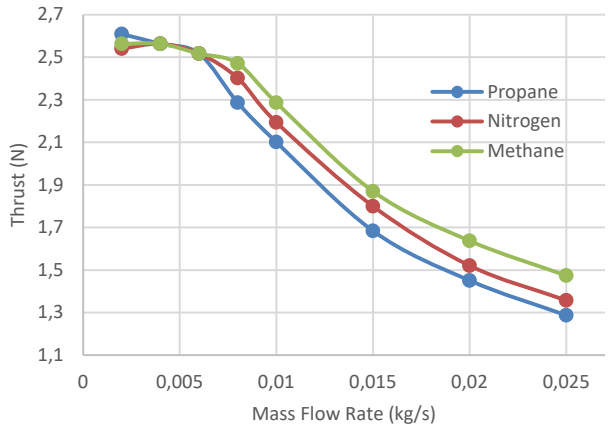

Fig. 9 Thrust vs. mass flow rate for the MPD thruster with a constant nozzle (L_Z = 3.02)

TABLE VII
EXPERIMENT RESULTS FOR THE MPD THRUSTER WITH A DIVERGENT NOZZLE (L_Z = 1.42)

P	$\dot{m}$ (kg/s)	θ	T (N)	u_e (m/s)	I_{sp} (s)
Propane (C_3H_8)	0.002	16.6	3.837410	1918.7050	195.58665
	0.004	16.6	3.837410	959.35252	97.793325
	0.006	16.4	3.792453	632.07564	64.431768
	0.008	15	3.476497	434.5621	44.297875
	0.01	14	3.249532	324.9532	33.124690
	0.015	12.4	2.884357	192.29053	19.601481
	0.02	11.4	2.654963	132.74819	13.531925
	0.025	10	2.332469	93.29876	9.5105771
Nitrogen (N_2)	0.002	16.6	3.837410	1918.7050	195.58665
	0.004	16.4	3.792453	948.11347	96.647652
	0.006	16.4	3.792453	632.07564	64.431768
	0.008	15.7	3.634746	454.34335	46.31430
	0.01	14.8	3.431186	343.118672	34.976419
	0.015	12.9	2.998729	199.915327	20.378728
	0.02	11.5	2.677940	133.89703	13.649035
	0.025	10.1	2.355552	94.222113	9.6047006
Methane (CH_4)	0.002	16.8	3.882319	1941.1597	197.87561
	0.004	16.6	3.837410	959.35252	97.793325
	0.006	16.5	3.814937	635.82296	64.813758
	0.008	16	3.702403	462.80042	47.176393
	0.01	15.3	3.544383	354.43834	36.130309
	0.015	13.3	3.090063	206.00423	20.999411
	0.02	12	2.792701	139.63509	14.233954
	0.025	11	2.562975	102.51903	10.45046

IV. CONCLUSION

MPD thrusters were investigated in the present study through theoretical and experimental research. Moreover, their performance was analyzed when using two different exhaust geometries. Various propellants and various inlet $\dot{m}$ values were used. The findings indicate that the MPD thruster with a divergent nozzle performs better than that with a constant nozzle.

At the end of the experiment, it was observed that the electrodes of the thruster eroded. Thus, the erosion effect can be investigated in the future.

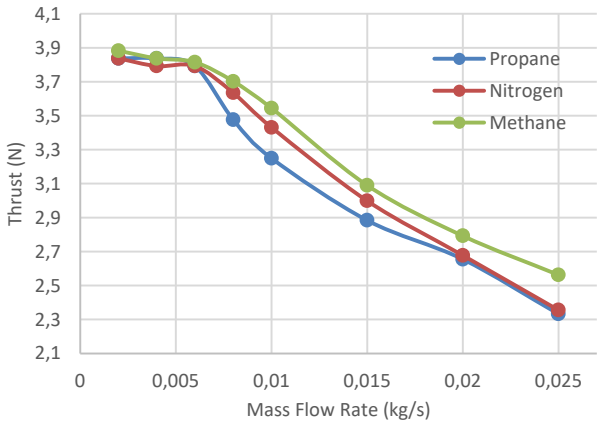

Fig. 10 Thrust vs. mass flow rate for the MPD thruster with a divergent nozzle (L_Z = 1.42)

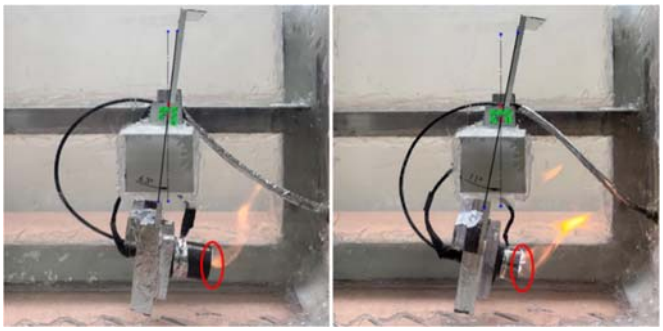

Fig. 11 Current density when using methane and when $\dot{m}$ = 0.025 kg/s

ACKNOWLEDGMENTS

A. Almuwallad thanks his academic advisors, Dr. Akram Muhammad and Dr. Khaled Al-Juhani, for their guidance in completing this paper.

REFERENCES

[1] R. G. Jahn, "Physics of Electric Propulsion," vol. 36, Third Ed. New York: Courier Dover Publications, pp. 8–255, 1968.
[2] G. P. George, P. Sutton, and O. Biblarz, "Rocket Propulsion Elements," Seventh Ed. New York: John Wiley & Sons, 2001.
[3] D. M. Goebel, and I. Katz, "Fundamentals of Electric Propulsion: Ion and Hall Thrusters," California: JPL Space Science and Technology Series, 2008.
[4] A. Villar, "Fluid Modelling of Magnetoplasmadynamic Thrusters," 2014.
[5] M. Ahmer, "Estimation and Comparison of Thrust for Self-Field MPD Thrusters," *Int. J. Sci. Eng. Res.*, vol. 7, pp. 1580–1584, 2016.
[6] J. A. Bittencourt, "Fundamentals of Plasma Physics," Third Ed. Brazii: Springer, 2004.
[7] V. Botti, "Theoretical Study of an MPD Thruster," Veneto: University Degli Studi di Padova, 2017. Accessed: Feb. 02, 2022.
[8] C. A. B. Stoute, "Design and Implementation of Low-Power Low-Cost Quasi Steady-State Magnetoplasmadynamic Propulsion Using Ar-He and N2-He Gas Mixtures," *Int. J. Aerosp. Syst. Sci. Eng.*, vol. 1, 2021.
[9] H. Kizmaz, S. Aksoy, and A. Muhurcu, "Sliding Mode Control of Suspended Pendulum," *Proc. - Int. Symp. Mod. Electr. Power Syst.*, 2010.